consequently it is expected that the deprotonated form, tris(thiohydroximato)ferrate(III), would display spin-crossover behavior, if it occurred, at a relatively higher temperature than the corresponding neutral species. We have found such behavior for the tris(hydroxamato)cobalt(III) and tris(hydroximato)cobaltate(III) salts;[24] however, the $\mu_{eff}$ values of *both* the neutral and the trianionic forms of tris(thiobenzohydroxamato)iron(III) remain constant down to ~5 K.

In summary, results of this study show that (1) both the hydroxamate and the thiohydroxamate complexes of ferric ion, as well as the corresponding deprotonated hydroximate and thiohydroximate complexes, show reversible or quasi-reversible electrochemical behavior under suitable conditions, (2) deprotonation of the hydroxamate complex stabilizes the Fe(III) vs. the Fe(II) state, (3) the replacement of the carbonyl oxygen by sulfur stabilizes the Fe(II) state relative to the Fe(III) state (which makes biological iron release by reduction even easier for thiohydroxamate than for hydroxamate siderophores), and (4) the thiohydroxamate and thiohydroximate complexes of Fe(III) display high-spin magnetic moments down to 5 K.

**Acknowledgment.** This research is supported by the NIH. We thank Dr. Norman Edelstein for experimental assistance with the magnetic susceptibility measurements and the U.S. AID for a fellowship to K.A.-D.

**Registry No.** Tris(acethydroxamato)iron(III), 14587-53-2; Fe(thiobenzohydroxamato)$_3$, 31375-72-1; $[Co(en)_3][Fe(thiobenzohydroximato)_3]$, 68024-55-5; sodium tris(benzohydroximato)ferrate(III), 23683-81-0; tris(*N*-methylbenzohydroxamato)iron(III), 68024-56-6; tris(*N*-methylthiobenzohydroxamato)iron(III), 68069-75-0.

## References and Notes

(1) Part 14 in this series: K. Abu-Dari, J. D. Ekstrand, D. R. Freyberg, and K. N. Raymond, *Inorg. Chem.*, in press.
(2) J. B. Neilands, "Inorganic Biochemistry", G. Eichhorn, Ed., Elsevier, New York, N.Y., 1973, p 167.
(3) C. E. Lankford, *Crit. Rev. Microbiol.*, **2**, 273 (1973).
(4) J. B. Neilands, Ed., "Microbial Iron Metabolism", Academic Press, New York, N.Y., 1974.
(5) J. Leong and K. N. Raymond, *J. Am. Chem. Soc.*, **96**, 6628 (1974).
(6) J. Leong and K. N. Raymond, *J. Am. Chem. Soc.*, **97**, 293 (1975).
(7) S. S. Isied, G. Kuo, and K. N. Raymond, *J. Am. Chem. Soc.*, **98**, 1763 (1976).
(8) S. Itoh, K. Inuzuka, and T. Suzuki, *J. Antibiot.*, **23**, 542 (1970).
(9) Y. Egawa, K. Umino, S. Awataguchi, Y. Kawano, and T. Okuda, *J. Antibiot.*, **23**, 267 (1970).
(10) S. R. Cooper, J. V. McArdle, and K. N. Raymond, *Proc. Natl. Acad. Sci.*, **75**, 3551 (1978).
(11) H. Bickel, G. E. Hall, W. Keller-Schierlein, V. Prelog, E. Vischer, and A. Wettstein, *Helv. Chim. Acta*, **43**, 2129 (1960).
(12) A. J. Mitchell, K. S. Murray, P. J. Newman, and P. E. Clark, *Aust. J. Chem.*, **30**, 2439 (1977).
(13) K. Nagata and J. Mizukami, *Chem. Pharm. Bull.*, **15**, 61 (1967).
(14) R. Dietzel and Ph. Thomas, *Z. Anorg. Allg. Chem.*, **381**, 214 (1971).
(15) L. M. Epstein and D. K. Straub, *Inorg. Chem.*, **8**, 453 (1969).
(16) K. Abu-Dari and K. N. Raymond, *Inorg. Chem.*, **16**, 807 (1977).
(17) H. St. Räde, *J. Phys. Chem.*, **77**, 424 (1973).
(18) F. E. Mabbs and D. J. Machin, "Magnetism and Transition Metal Complexes", Chapman and Hall, London, 1973.
(19) G. Anderegg, F. L'Eplattenier, and G. Schwarzenbach, *Helv. Chim. Acta*, **44**, 1400 (1963).
(20) R. Nicholson and I. Shain, *Anal. Chem.*, **36**, 706 (1964).
(21) L. Meites, "Polarographic Techniques", Wiley, New York, N.Y., 1965, p 279.
(22) W. M. Latimer, "Oxidation States of the Elements and Their Potentials in Aqueous Solution", 2nd ed., Prentice-Hall, Inc., Englewood Cliffs, N.J., 1952.
(23) L. Cambi, T. Bacchetti, and E. Paglia, *Rend., Ist. Lomb. Accad. Sci. Lett. A*, **90**, 577 (1956).
(24) K. Abu-Dari and K. N. Raymond, to be submitted for publication.

---

Contribution from the Department of Chemistry, Texas A&M University, College Station, Texas 77843

# Electronic Structure of Mixed-Valence Ions: ESCA and MO Calculations on $[\eta^5\text{-}C_5H_5Fe(CO)]_2\text{-}\mu\text{-}Ph_2P(CH_2)_nPPh_2^{m+}$ ($n$ = 1, 2; $m$ = 0, 1)

DAVID E. SHERWOOD, JR., and MICHAEL B. HALL*

*Received April 18, 1978*

The ESCA spectra of the title compounds are presented and compared to the results of parameter-free Fenske–Hall molecular orbital calculations. The calculations are used both to calculate ESCA satellite intensities via the sudden approximation and to describe the valence electronic structure. The results of the sudden approximation, which predict no satellites of intensity greater than 10% of the main peak, are in good agreement with the ESCA spectra, where no satellites are discernible. However, using the same theoretical results, we find that the Hush model predicts a single intense satellite, which is in disagreement with the full MO sudden approximation and the ESCA spectra. The description of the valence electronic structure is in good agreement with previous results for the cyclic voltammetry, for the carbonyl stretching frequencies, and for the crystal structures. However, they suggest that oxidation of the neutral species involves removal of an Fe–Fe nonbonding electron rather than removal of an electron from the Fe–Fe $\sigma$ bond.

## Introduction

The dimers $[CpFe(CO)]_2Ph_2P(CH_2)_nPPh_2^{m+}$ ($n$ = 1, 2; $m$ = 0, 1) (Cp = $\eta^5$-$C_5H_5$, Ph = $C_6H_5$) have been synthesized and characterized by Haines and du Preez.[1] These compounds, which have a bridging diphosphine group and two bridging carbonyls, possess approximate $C_{2v}$ symmetry, as shown in Figure 1. The neutral species are thought to have a single Fe–Fe bond, while the oxidized species are thought to have a one-electron Fe–Fe bond.[1,2] Thus, these latter species would be delocalized mixed-valence complexes (class IIIa in the terminology of Robin and Day[3]).

Although one might expect a delocalized mixed-valence metal dimer to show a single metal ESCA peak and a localized dimer (class II) to show two metal ESCA peaks, Hush has suggested that a delocalized dimer could have an ESCA spectrum like that of a localized dimer.[4] According to Hush, the ionization of a core electron on the metal will cause the formally delocalized valence electron to localize on one of the two metal centers (now differing by a core electron). The ratio of the intensity of the peak at low binding energy to that at high binding energy is proportional to the electronic coupling integral ($J$ in Hush's notation). Thus, for strongly coupled metal centers one might expect a main ESCA peak and a weaker satellite, while for weakly coupled metals (but still delocalized) one would expect to see two nearly equal ESCA peaks.

In this work we have examined the ESCA spectra of the title compounds to test Hush's model for rather strongly

0020-1669/78/1317-3397$01.00/0 

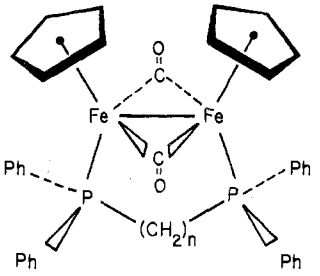


**Figure 1.** Structure of $[CpFe(CO)]_2Ph_2P(CH_2)_nPPh_2^{m+}$ ($n$ = 1, 2; $m$ = 0, 1).

coupled metal centers (direct metal–metal bond). We will also compare the results of this model to complete molecular orbital (MO) calculations and theoretical satellite intensities calculated via the sudden approximation.[5] The MO calculations have also been used to interpret the cyclic voltammetry,[6] the change in $\nu_{CO}$ on oxidation,[1] and the crystal structure of the oxidized and unoxidized dimers.[7] The cyclic voltammogram for the unoxidized species shows a reversible oxidation followed by an irreversible one, which results in asymmetric cleavage of the dimer.[6] Ferguson and Meyer[6] suggest that these oxidations involve successive removal of one and then two electrons from the metal–metal bond. However, this is difficult to reconcile with the large change in $\nu_{CO}$ upon oxidation,[1] since one would not expect a strong interaction between the metal–metal $\sigma$ bond and the carbonyl $2\pi$ orbitals. Furthermore, the crystal structure shows only a small change in the Fe–Fe distance upon oxidation, while the changes in the Fe–P distances are larger.[7]

## Experimental Section

**Preparation.** Dicyclopentadienyldiiron tetracarbonyl, $[CpFe(CO)_2]_2$, was obtained from Strem Chemicals and recrystallized from aqueous pyridine.[8] The substituted diphosphine derivatives, $[CpFeCO]_2Ph_2P(CH_2)_nPPh_2$ ($n$ = 1, 2), and their tetraphenylborate salts, were synthesized by the methods of Haines and du Preez.[1] The neutral compounds were purified by recrystallization from benzene. After oxidation with iodine, the salts were washed with copious amounts of toluene and repeatedly recrystallized from dichloromethane–pentane.

**Spectra.** X-ray photoelectron spectra of the solids were recorded on a Hewlett-Packard 5950 A ESCA spectrophotometer. This instrument has a resolution of 0.2 eV. A flood gun providing low-energy electrons was used to eliminate surface charging. Samples were maintained at 290 K. The pressure in the analyzer was less than $2 \times 10^{-9}$ torr. Degradation of the spectra of all compounds was noted at prolonged exposure times (ca. 6 h at 800 W).

## Theoretical Calculations

**MO Calculations.** Fenske–Hall molecular orbital calculations[9] (parameter-free, self-consistent field) were performed on an Amdahl 470 V/6 computer. Atomic positions for an idealized $C_{2v}$ geometry were based on the crystal structure of $[CpFe(CO)_2]_2$[10] and $Fe_2$(diphos) geometries of related compounds.[11] The general features of the MO's will be insensitive to small errors in atomic positions. The transition-metal atomic functions were those of Richardson[12] for $Fe^+$ with 4s and 4p exponents of 2.0.[13] The C, O, and P functions were the double-$\zeta$ functions of Clementi,[14] and all but the outer p orbitals were reduced to single-$\zeta$ functions.[15] An exponent of 1.2 was used for all hydrogens. In the actual calculations the phenyl rings attached to the P were replaced by hydrogens. This substitution should have only a small effect on the higher energy, mainly metal, orbitals.

**Satellite Calculations.** Hush expresses the ratio of the intensity of the main peak ($I_m$) to the intensity of the satellite ($I_s$) as

$$I_m/I_s = [(1 + (1 + \alpha^2)^{1/2} + \alpha)/(1 + (1 + \alpha^2)^{1/2} - \alpha)]^2 \quad (1)$$

where

$$\alpha = 2J/\Delta \quad (2)$$

$2J$ is the intervalence transfer energy of the delocalized system (before core ionization), and $\Delta$ is the intervalence transfer energy of the localized system (after core ionization).[4] We have calculated $2J$ and $\Delta$ from the differences in the orbital energies. Although this procedure is only approximate, it should yield a reasonable ratio ($\alpha$).

In the calculation of the satellites with the sudden approximation, we have followed the approach of Aarons, Barber, Guest, Hillier, and McCartney.[16] The ground-state wave function for the un-ionized molecule ($n$ electrons) is

$$\Phi_0 = |\mu_1\mu_2\mu_3...\mu_n| \quad (3)$$

where $\mu_i$ is the molecular spin orbital for the $i$th electron. The core-hole wave function, in which an electron is removed from the core orbital $\mu_1$, is

$$\Phi_1 = |\mu_2\mu_3...\mu_n| \quad (4)$$

The ground-state wave function for the core-hole ion, in which the orbitals are allowed to relax, is

$$\Psi_0 = |\nu_2\nu_3...\nu_{i-1}\nu_i\nu_{i+1}...\nu_n| \quad (5)$$

where the spin orbitals $\nu_i$ are now different from those in eq 4. Excited states of the core-hole ion (shake-up) can be represented by the wave function

$$\Psi_{i\rightarrow j} = |\nu_2\nu_3...\nu_{i-1}\nu_j\nu_{i+1}...\nu_n| \quad (6)$$

The probability of a transition to $\Psi_0$ upon ionization of the core electron is

$$P_0 = |\langle\Phi_1|\Psi_0\rangle|^2 \quad (7)$$

while the probability of a transition to $\Psi_{i\rightarrow j}$ is

$$P_{i\rightarrow j} = |\langle\Phi_1|\Psi_{i\rightarrow j}\rangle|^2 \quad (8)$$

The total probability of secondary excitation (both shake-up and shake-off) is $(1 - P_0)$. The integrals in eq 7 and 8 are the overlap integrals between determinantal wave functions of nonorthogonal orbitals. The value for such an integral is the determinant of the molecular orbital overlaps $\langle\mu_k|\nu_1\rangle$.

The MO procedure described previously is used to construct the wave functions using the same atomic orbital basis for both $\mu_k$ and $\nu_1$. Previous work[17] has shown that most of the relaxation upon core ionization occurs in the more mobile valence electrons. We have assumed that the core functions are unchanged upon ionization and that the relaxed core-hole state can be well represented by the equivalent core model.[18] This involves increasing the core charge on the atom of interest by 1 to simulate the ESCA experiment. These assumptions will introduce an error in the absolute probabilities, but they should not alter the trends in the probabilities.

## Results

**ESCA Spectra.** Figure 2 shows the ESCA spectrum of $[CpFe(CO)]_2Ph_2PCH_2PPh_2^+$ in the Fe $2p_{3/2,1/2}$ region. There are no discernible satellites in the spectra of either compound ($m$ = 0, 1) nor were there any in the ethyl analogues. Table I lists the binding energies and full width at half-maximum (fwhm) values of the Fe 2p, Fe 3s, and P 2p peaks for all of the compounds studied relative to C 1s (285.0 eV). The C peaks were somewhat broader than standard graphite (0.2 eV), due to the wide variety of C atoms in the sample. The peak positions are reproducible to better than 0.2 eV. Although the shifts are rather small, they appear to be toward higher binding energy for the oxidized species. The fwhm of the ethyl derivative peaks are slightly broader than their methyl analogues. There is a more significant broadening of all peaks

**Table I.** Position and Fwhm Values (eV) for $[CpFe(CO)]_2Ph_2P(CH_2)_nPPh_2^{m+}$ ESCA Results[a]

| | I | | II | | III | | IV | |
|---|---|---|---|---|---|---|---|---|
| | position | fwhm | position | fwhm | position | fwhm | position | fwhm |
| Fe $2p_{3/2}$ | 708.4 | 1.17 | 708.7 | 1.56 | 708.3 | 1.37 | 708.7 | 1.95 |
| Fe $2p_{1/2}$ | 721.2 | 1.56 | 721.6 | 2.34 | 721.0 | 1.76 | 721.4 | 2.73 |
| Fe $3s_{1/2}$ | 54.8 | 2.34 | 55.0 | 2.73 | 54.4 | 2.58 | 55.3 | 3.34 |
| P $2p_{3/2,1/2}$ | 131.3 | 1.40 | 131.3 | 1.56 | 131.1 | 1.56 | 131.3 | 2.03 |

[a] I, $n = 1$, $m = 0$; II, $n = 1$, $m = 1$; III, $n = 2$, $m = 0$; IV, $n = 2$, $m = 1$.

**Table II.** Results of Fenske-Hall MO Calculations for $[CpFe(CO)]_2H_2PCH_2PH_2^+$ Showing the Percent Character of the Atomic or Molecular Basis Constituents[a]

| | | % character (total) | | | | | | | | | | | |
|---|---|---|---|---|---|---|---|---|---|---|---|---|---|
| | | Fe | | | CO | | | Cp | | | P lone pairs | | main Fe-Fe interactions |
| MO | orbital energy, eV | 4s | 4p | 3d | $1\pi$ | $5\sigma$ | $2\pi$ | $1a_1''$ | $1e_1''$ | $1e_2''$ | $a_1$ | $b_2$ | |
| $19a_1$ | −5.67 | | 8 | 42 | | 4 | 14 | | 24 | | 5 | | $\sigma, \delta$ |
| $15b_2$ | −9.24 | 2 | 6 | 64 | | | 14 | | 10 | | | | $\sigma^*$ |
| $8a_2$ | −13.32 | | 14 | 49 | 3 | | 20 | | 12 | 1 | | | $\delta^*$ |
| $14b_2$ | −13.83 | | 2 | 94 | | | | 1 | | 1 | | | $\pi^*$ |
| $13b_1$ | −14.24 | | 8 | 62 | 2 | 2 | 8 | | 13 | 2 | | | $\delta, \pi$ |
| $18a_1$ | −14.81 | | 3 | 87 | | | 1 | | 5 | 1 | | | $\sigma, \delta$ |
| $7a_2$ | −15.27 | | 1 | 68 | 9 | | 18 | | 1 | 2 | | | $\delta^*, \pi^*$ |
| $17a_1$ | −15.46 | | 2 | 79 | 4 | | 11 | | | 2 | 1 | | $\pi$ |
| $13b_2$ | −15.61 | 4 | 1 | 51 | 15 | | 27 | | | 1 | | | $\sigma^*, \delta^*$ |
| $12b_2$ | −17.95 | | 5 | 19 | | | | | 71 | | | 2 | $\sigma^*, \delta^*$ |
| $12b_1$ | −18.01 | | 2 | 23 | 5 | 1 | 2 | | 64 | | | | $\delta, \pi$ |
| $16a_1$ | −18.11 | | 4 | 17 | 2 | 3 | 2 | | 68 | | 2 | | $\sigma$ |
| $6a_2$ | −18.13 | | 1 | 31 | | | | | 64 | | | | $\delta^*, \pi^*$ |
| $15a_1$ | −20.89 | | 7 | 24 | 5 | 3 | | 11 | 1 | | 45 | | $\sigma, \delta$ |
| $10b_2$ | −21.48 | 1 | 10 | 14 | 2 | | | 24 | | | | 47 | $\sigma^*, \delta^*$ |

[a] $8a_2$ is the highest occupied molecular orbital (HOMO).

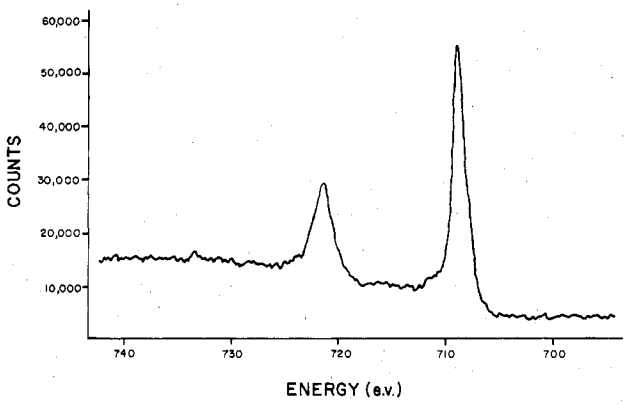


**Figure 2.** ESCA spectrum of $[CpFe(CO)]_2Ph_2P(CH_2)Ph_2BPh_4$ in the Fe $2p_{3/2,1/2}$ region.

upon oxidation of the compounds. The Fe $3s_{1/2}$ peaks show the most dramatic broadening but are of low intensity because longer counting times lead to degradation of the spectra.

**MO Calculations.** Using the Fenske–Hall approach and the wave functions described previously, we performed MO calculations on $[CpFe(CO)]_2H_2PCH_2PH_2^{m+}$ ($m = 0, 1$) and on the core-hole states of these two species using the equivalent core approximation. Table II lists the results for the mixed-valence dimer ($m = 1$). The $C_{2v}$ symmetry labels (column 1) are numbered beginning with the first valence molecular orbital. The body of the table lists the major character of each molecular orbital in terms of the atomic iron orbitals and the free ligand molecular orbitals. The last column indicates the type of Fe–Fe interaction in terms of a diatomic $Fe_2$ moiety.

The highest occupied molecular orbital (HOMO) is the $8a_2$ orbital, which is $\delta^*$ with respect to the Fe–Fe interaction and also contains substantial CO $2\pi$ character. However, this orbital is essentially nonbonding as can be seen in Figure 3a. The $14b_2$ orbital consists almost entirely of Fe $d_{yz}$ ($\pi^*$) character. The $13b_1$ orbital (Figure 3b) is the $\delta$ counterpart

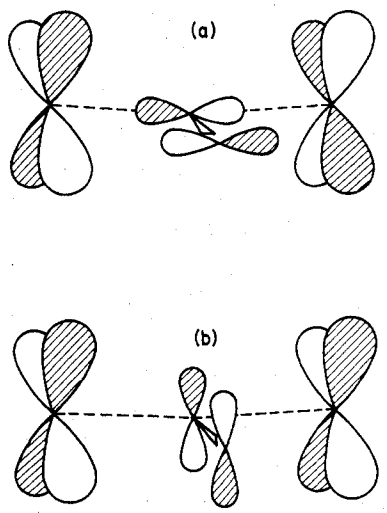


**Figure 3.** Iron–carbonyl–iron orbital contributions to the $8a_2$ (a) and $13b_1$ (b) orbitals. The $8a_2$ orbital, the HOMO, is essentially nonbonding and is the orbital from which an electron is removed upon oxidation. The $13b_1$ orbital is the corresponding bonding orbital and forms part of the Fe–CO–Fe framework bond. Only one carbonyl is shown; the second carbonyl is below the plane of the paper and has C and O orbitals of opposite sign.

of the $8a_2$, $\delta^*$, orbital. The cyclopentadienyl interactions are Fe–Cp bonding in the $13b_1$ orbital but antibonding in the $8a_2$ orbital. The intervalence transfer would correspond to the $13b_1 \rightarrow 8a_2$ transition. The major contribution to the Fe–Fe $\sigma$ bond arises in the $18a_1$ MO. The $\sigma^*$ orbital is readily identified as $15b_2$, which is the lowest unoccupied molecular orbital (LUMO). The $7a_2$, $17a_1$, and $13b_2$ orbitals are involved primarily in the Fe–CO–Fe bridge bonding. The $12b_2$, $12b_1$, $16a_1$, and $6a_2$ orbitals constitute the Cp–Fe bond (formally $Cp^-$ to $Fe^+$ donation). The Fe–P bonds are localized in the $16a_1$ and $10b_2$ orbitals.

In order to obtain the relaxed wave function for the intensity calculations, we increased by 1 the effective nuclear charge of one iron (equivalent core). The symmetry is now reduced to $C_s$, where $a_1$ and $b_2$ become a′ and $b_1$ and $a_2$ become a″. There is considerable relaxation of the valence electrons toward the iron with the hole, which we will denote as Fe*. The HOMO is now localized on the Fe which was not photoionized, with a character of 35% Fe and 3% Fe*. Lower in energy by 6.2 eV is the corresponding orbital which is localized on the Fe* atom.

Calculations were also done on the neutral complex ($m$ = 0). The general orbital structure is similar to that of the mixed-valence ion ($m$ = 1). The HOMO in the neutral complex is 58% 3d Fe, 12% 4p Fe, 16% $2\pi$ CO, and 8% $1e_1''$ Cp. Although one might expect removal of an electron from the HOMO (oxidation) to reflect considerable loss of Fe electron density, the Fe charge (Mulliken population analysis) only changes from +0.43 to +0.47 upon oxidation. This type of comparison for all of the atoms leads to the conclusion that loss in electron density is 50% Cp, 26% CO, 15% diphos, and 9% Fe. Thus, the valence electron density relaxes upon oxidation of the metal center, which results in little loss of metal charge because of compensation by ligand donation. We have also examined the changes in overlap population (proportional to bond order) upon oxidation. These results suggest only a small change in the Fe–Fe bond, while both the C–O and Fe–Cp bonds were strengthened and both the Fe–CO and Fe–P bonds were weakened.

**Satellite Calculations.** In the Hush model, $2J$ corresponds to the $13b_1 \rightarrow 8a_2$ transition of the delocalized mixed-valence dimer, while $\Delta$ corresponds to the analogous transition in the localized core-hole state. Our theoretical calculations give $2J$ = 0.92 eV and $\Delta$ = 6.17 eV. Thus, $\alpha$ = 0.15 (eq 2) and the ratio of the intensity of the main to satellite would be 1.35 (eq 1). If we give the main peak an arbitrary intensity of 100%, the satellite would be predicted to be 74% of the main peak intensity.[19] Thus, with our theoretical results the Hush model predicts a very large satellite.

We have also used our theoretical results in the sudden approximation. We considered all possible symmetry-allowed ($C_s$) transitions from the 15 lowest energy filled orbitals to the seven lowest energy empty orbitals. This resulted in the calculation of 54 probabilities (eq 8), each of which involved the evaluation of a 53 × 53 determinant. Excitations from lower energy occupied MO's would involve satellites outside the Fe $2p_{3/2,1/2}$ region studied. For the neutral dimer ($m$ = 0), no excitations in this range produced satellite intensities greater than 1%. The absolute probability of the main peak was 84%, which suggests that 16% of the intensity is lost to high-energy satellites or to multiple ionizations (shake-off). For the mixed-valence dimer the absolute probability of the main peak was 61%; thus, 39% of the intensity must be lost to shake-up or shake-off. In this case four excitations produced satellites with intensities greater than 1%. The three strongest were all excitations from doubly filled orbitals to the singly occupied HOMO and had intensities of 9.4, 5.6, and 3.9%. The strongest of these corresponds to the hole localizing on one or the other Fe atoms, in qualitative agreement with the Hush model. The other two correspond to transitions from orbitals localized on the same atom as the HOMO and from orbitals delocalized over both Fe atoms, respectively.

## Discussion

The ESCA spectra showed only small shifts in the Fe and P peaks upon oxidation. These results are consistent with our equivalent core MO calculations, which suggest that, although initially the MO from which the electron is removed on oxidation is ~50% Fe, the system relaxes in such a manner that the Fe charge is nearly constant. The increase in the fwhm can be explained as unresolved multiplet splitting.

Neither the neutral dimer nor the mixed-valence ion show any satellite structure. For the neutral dimer this result is in agreement with the results of the sudden approximation. For the mixed-valence ion the sudden approximation predicts two satellites with intensities greater than 5% and two more with intensities between 4 and 2%. Considering the very approximate nature of the calculation, we believe this discrepancy is very minor. The sudden approximation may be predicting intensities which are in error by a factor of 2–3, in which case they could be easily lost in the background counts. Alternatively, if they are broad and overlapping in the spectra, they could easily have intensities as large as those predicted and still not be observed.

More disconcerting is the disagreement of the Hush model with the full sudden approximation, when the same MO calculations are used in both. The Hush model predicts a satellite which is nearly 74% of the main peak, in clear disagreement with both the experimental and sudden approximation results. The problem with the Hush model is that it only considers the change in character of two orbitals upon core ionization. Thus, all of the intensity arising from the relaxation to the main peak will appear in one satellite. The full MO sudden approximation predicts a main peak of absolute intensity 61%. If all of the intensity lost (39%) were to appear in a single peak, it would have an intensity of 63% of the main peak, a result in close agreement with the Hush model. Apparently, the Hush model, which will always predict a single satellite, is simply inappropriate for these strongly coupled metal systems, where a more complete treatment suggests several weak, possibly unobservable satellites, in agreement with the experiment. We have also noted rather large ligand involvement in the molecular orbitals that give rise to the calculated satellite intensities in these systems, in direct contrast to the simplification used in the Hush model.

The MO calculations are also in agreement with other experimental results, although not always with the previous interpretations. In previous work[1,2] it was assumed that oxidation of the neutral species resulted in removal of one electron from the Fe–Fe $\sigma$ bond. Further oxidation to the $m$ = 2+ species would then disrupt the Fe–Fe $\sigma$ bond and, as is observed in the cyclic voltammogram, lead to decomposition. Our calculation suggests that the HOMO is not Fe–Fe $\sigma$ bonding but Fe–Fe nonbonding. Calculations on the oxidized species show that removal of an electron from the HOMO results in a weakening of the bridging ligand to Fe bonds (Fe–CO and Fe–P). If removal of a second electron further weakens this bridging system, the Fe–Fe $\sigma$ interaction may not be strong enough to maintain the dimer intact. This explanation is consistent with the crystallographic results[7] which show changes of less than 0.01 Å in the Fe–Fe distance upon oxidation, but somewhat larger changes in the Fe–P distance (~0.04 Å).

Comparison of the MO's of the neutral and oxidized species also suggests considerable electron density loss from the carbonyl $2\pi$ system upon oxidation, which should strengthen the C–O bond. This is reflected in the substantial change in carbonyl stretching frequency upon oxidation (1719 and 1678 $cm^{-1}$ to 1835 and 1780 $cm^{-1}$ for the ethyl analogue).[1]

In conclusion, we believe our theoretical results are in good agreement with both our ESCA results and previous experimental results and yield a consistent picture of the electronic structure of these mixed-valence dimers. The results also suggest some caution in the indiscriminate application of Hush's model for the effects of relaxation on mixed-valence dimers.

**Acknowledgment.** The authors thank the Robert A. Welch Foundation (Grant A-648) for support of this work, Drs. K.

Hardcastle and R. Mason for communicating their results prior to publication, and Ms. E. Boespflug for preparation of some of the complexes.

**Registry No.** $[CpFeCO]_2Ph_2P(CH_2)PPh_2$, 60508-02-3; $\{[CpFeCO]_2Ph_2P(CH_2)PPh_2\}BPh_4$, 12701-56-3; $[CpFeCO]_2Ph_2P(CH_2)_2PPh_2$, 12701-59-6; $\{[CpFeCO]_2Ph_2P(CH_2)_2PPh_2\}BPh_4$, 12701-60-9.

## References and Notes


(1) (a) R. J. Haines and A. L. du Preez, *J. Organomet. Chem.*, **21**, 181 (1970); (b) R. J. Haines and A. L. du Preez, *Inorg. Chem.*, **11**, 330 (1972).
(2) T. J. Meyer, *Prog. Inorg. Chem.*, **19**, 1 (1975).
(3) M. B. Robin and P. Day, *Adv. Inorg. Radiochem. Chem.*, **10**, 248 (1967).
(4) N. S. Hush, *Chem. Phys.*, **10**, 361 (1975).
(5) T. Åberg, *Phys. Rev.*, **156**, 35 (1969); *Ann. Acad. Sci. Fenn., Ser. A6*, **308**, 1 (1969).
(6) J. A. Ferguson and T. J. Meyer, *Inorg. Chem.*, **11**, 631 (1972).
(7) K. Hardcastle and R. Mason, private communication.
(8) B. F. Hallam and P. L. Pauson, *J. Chem. Soc. A*, 3030 (1956).
(9) R. F. Fenske and M. B. Hall, *Inorg. Chem.*, **11**, 768 (1972).
(10) O. S. Mills, *Acta Crystallogr.*, **11**, 620 (1958).
(11) F. A. Cotton and J. M. Troup, *J. Am. Chem. Soc.*, **96**, 4422 (1974).
(12) J. W. Richardson, W. C. Nieuwpoort, R. R. Powell, and W. F. Edgell, *J. Chem. Phys.*, **36**, 1057 (1962).
(13) M. Barber, J. A. Connor, M. F. Guest, M. B. Hall, I. H. Hillier, and W. N. E. Meredith, *Faraday Discuss. Chem. Soc.*, **54**, 219 (1972).
(14) "Tables of Atomic Functions", a supplement to a paper by E. Clementi, *IBM J. Res. Dev.*, **9**, 2 (1965).
(15) D. D. Radtke, Ph.D. Thesis, University of Wisconsin, 1966.
(16) L. J. Aarons, M. Barber, M. F. Guest, I. H. Hillier, and J. H. McCartney, *Mol. Phys.*, **26**, 1247 (1973).
(17) L. J. Aarons, M. F. Guest, M. B. Hall, and I. H. Hillier, *J. Chem. Soc., Faraday Trans.*, 563 (1973).
(18) W. L. Jolly and D. N. Hendrickson, *J. Am. Chem. Soc.*, **92**, 1863 (1970); J. M. Hollander and W. L. Jolly, *Acc. Chem. Res.*, **3**, 193 (1970).
(19) A reviewer has suggested that one should not identify the two orbitals of Hush's model with particular orbitals of a full MO calculation but rather with the average value of the manifold of bonding and antibonding orbitals, respectively. The main metal–metal bonding orbitals are $13b_1$, $18a_1$, and $17a_1$, and the main metal–metal antibonding orbitals are $15b_2$, $8a_2$, and $14b_2$. Averaging these groups of orbitals, we obtained $2J$ = 2.71 eV. Applying a similar averaging to the core-hole state, we obtained $\Delta$ = 5.57 eV. The satellite is then predicted to be 40% of the main peak.


Contribution from the Department of Chemistry, University of Missouri—Rolla, Rolla, Missouri 65401

# Mössbauer, Electronic, and Structural Properties of Several Bis- and Tetrakis(pyridine)iron(II) Complexes

BILL F. LITTLE and GARY J. LONG*

*Received December 7, 1977*

The high-spin tetrakis(pyridine)iron(II) complexes $Fe(py)_4X_2$, where X is Cl, Br, I, NCO, NCS, and NCSe, have a tetragonally distorted trans octahedral structure. Magnetically perturbed Mössbauer spectra for each of these compounds indicate a positive electric field gradient tensor and a nondegenerate orbital ground term. An angular overlap analysis of the quadrupole interaction in these compounds indicates that, relative to chlorine and bromine and the pseudohalides, pyridine is a poor $\pi$-bonding ligand and is comparable to iodine. The high-spin pseudooctahedral $Fe(py)_2X_2$ complexes, where X is Cl, Br, NCO, NCS, and NCSe, have polymeric linear-chain structures with bridging anions and trans pyridine ligands. The thiocyanate and selenocyanate complexes have both nitrogen and sulfur or selenium coordinated to adjacent iron atoms whereas the cyanate anion bridges via a three-center bond at the nitrogen atom. The Mössbauer spectra of the bis(pyridine) chloride, thiocyanate, and selenocyanate complexes reveal spontaneously ordered one-dimensional ferromagnets at 4.2 and 1.3 K. The Mössbauer spectrum at 4.2 and 1.1 K reveals that $Fe(py)_2Br_2$ is paramagnetic. No spontaneous ordering is observed at 4.2 K in a 6-T applied field. The electronic spectra at room temperature and at 23 K for all of these complexes have been evaluated in terms of the angular overlap model. The results indicate that pyridine is a better $\sigma$-bonding ligand than the halide or pseudohalide ligands. In general, the monodentate nonbridging halides and pseudohalides are better $\sigma$-bonding ligands than are the bridging ligands. The infrared and powder X-ray diffraction results—which indicate many isomorphisms with the analogous cobalt and nickel complexes—are consistent with the above structural assignments. All evidence indicates that $Fe(py)_2I_2$ has a pseudotetrahedral structure.

## Introduction

The bis- and tetrakis(pyridine) complexes of iron(II) halides and pseudohalides provide a means to study the structural, magnetic, and electronic properties of a compound as a function of the iron–ligand bond. This paper, a continuation of our earlier work on $Fe(py)_2Cl_2$[1] and $Fe(py)_2(NCS)_2$,[2] reports an investigation of the chloro, bromo, iodo, cyanato, thiocyanato, and selenocyanato complexes with pyridine. The incentive for this further work results from the structural isomers possible for the bis complexes, the existence of a metamagnetic transition,[3,4] and a structural phase transition[5] in certain of these complexes, as well as their suitability for study by optical and Mössbauer spectral techniques. Although there have been many earlier Mössbauer effect,[6-15] magnetic,[6,8,16-18] infrared,[19] optical,[8,20,21] and thermal[10,11,14,15] studies of individual iron–pyridine complexes, this work represents the first unified study of the bonding in these complexes for a series of anions.

## Experimental Section

All operations were carried out in a Vacuum Atmospheres Inc. inert-atmosphere glovebox filled with nitrogen. Solid reagent grade chemicals were used without further purification. All solvents were dried and deoxygenated by standard laboratory procedures. Spectroscopic grade pyridine was either distilled under a steam of dry nitrogen or stored over a molecular sieve. Elemental analyses for all compounds are reported in Table I.[22]

**Preparation of Tetrakis(pyridine)iron(II) Complexes.** These complexes were prepared by modifications of previously reported procedures.[1,6,16,21,23] These compounds are stable for many months when stored in an inert atmosphere in the dark. More synthetic details are available elsewhere.[24]

**Preparation of Bis(pyridine)iron(II) Complexes.** $Fe(py)_2Cl_2$ was prepared directly according to method A described previously by Long et al.[1]

In the preparation of $Fe(py)_2Br_2$, 0.022 mol of bromine, dissolved in 25 mL of deoxygenated methanol, was slowly added to an excess of reduced iron powder, stirred for several hours, and filtered twice to remove all traces of iron. To this solution 0.045 mol of freshly distilled pyridine was slowly added with stirring. A yellow crystalline precipitate formed within several minutes and was filtered, washed with a 50% by volume solution of anhydrous methanol and diethyl ether, and dried for 1 h under a static vacuum.

$Fe(py)_2I_2$ was prepared by heating $Fe(py)_4I_2$ under vacuum at 82 °C for 8 h in an Abderhalden drying apparatus. During this heating, the bright yellow crystals of the tetrakis complex underwent a 25.28% weight loss, a 50.0% pyridine loss, and became light yellow.

$Fe(py)_2(NCO)_2$ was prepared from $Fe(py)_4(NCO)_2$ by two different thermolytic procedures. In the first, hydrogen gas (purified by passage over copper turnings and iron wool at 550 °C and then through a liquid nitrogen trap) was passed over $Fe(py)_4(NCO)_2$ in a reduction tube held at 88 °C for 16 h. The weight loss of 34.6% corresponded to

0020-1669/78/1317-3401$01.00/0 